

Elsevier Editorial System(tm) for Bone
Manuscript Draft

Manuscript Number:

Title: Towards New Material Biomarkers for Fracture Risk

Article Type: Full length article

Keywords: aging, bone quality, hydroxyapatite, osteoporosis, trabecular bone, X-ray diffraction

Corresponding Author: Dr. Charlene Greenwood,

Corresponding Author's Institution: Cranfield University

First Author: Charlene Greenwood

Order of Authors: Charlene Greenwood; John Clement ; Anthony Dicken ; Paul Evans ; Iain Lyburn; Richard M Martin; Keith Rogers; Nick Stone ; Peter Zioupos

Abstract: Osteoporosis is a prevalent bone condition, characterised by low bone mineral density and increased fracture risk. Currently, the gold standard for identifying osteoporosis and increased fracture risk is through quantification of bone mineral density (BMD) using dual energy X-ray absorption (DEXA). However, the risk of osteoporotic fracture is determined collectively by bone mass, architecture and physico-chemistry of the mineral composite building blocks. Thus DEXA scans alone inevitably fail to fully discriminate individuals who will suffer a fragility fracture. This study examines bone at both ultrastructure and microarchitectural levels to provide a detailed material view of bone, and therefore produce a more comprehensive model of osteoporotic fracture risk. Physico-chemical characterisation obtained through X-ray diffraction and infrared analysis indicated significant differences in apatite crystal chemistry and microstructure between fracture and non-fracture groups. Further, this study, through considering the potential correlations between the chemical biomarkers and microarchitectural properties of the bone, has investigated the premise that bone mechanical properties (e.g. fragility) are affected by physicochemical material features.

Suggested Reviewers: Eugenia (Éva) Valsami-Jones Professor
Chair in Environmental Nanoscience, School of Geography, Earth and
Environmental Sciences, Birmingham University
e.valsamijones@bham.ac.uk

Chris Hall Dr
Senior Scientist, Imaging and Medical Therapy, Australian Synchrotron
chris.hall@synchrotron.org.au

Tim Wess Professor
Executive Dean, Charles Sturt University
deanofscience@csu.edu.au

Opposed Reviewers:

Highlights

- Physicochemical properties assessed through XRD and FTIR for non-fracture and fracture human specimens.
- Significant differences in coherence length, 'a' axis lattice parameters and carbonate:phosphate ratios between the two groups.
- With age, an increase in the phosphate to amide ratio and the coherence length was observed.
- Mineral properties of bone at the ultrastructure level may influence the micro architectural properties of trabecular bone.
- Possible differences in the material quality between fracture males and females, as observed through tissue mineral density (TMD) values.

Towards New Material Biomarkers for Fracture Risk

C. Greenwood^a, J. Clement^b, A. Dicken^c, J.P.O. Evans^c, I. Lyburn^d, R.M. Martin^e, K. Rogers^a,
N. Stone^f and P. Zioupos^a

^a *Cranfield Forensic Institute, Cranfield University, Defence Academy of the UK, Shrivenham, UK.*

^b *Forensic Odontology, Melbourne Dental School, University of Melbourne, Melbourne, Australia.*

^c *The Imaging Science Group, Nottingham Trent University, Nottingham, UK.*

^d *Cobalt Health, Cheltenham, UK.*

^e *Social and Community Medicine, Bristol University, Bristol, UK.*

^f *Physics and Astronomy, Exeter University, Exeter, UK.*

Abstract

Osteoporosis is a prevalent bone condition, characterised by low bone mineral density and increased fracture risk. Currently, the gold standard for identifying osteoporosis and increased fracture risk is through quantification of bone mineral density (BMD) using dual energy X-ray absorption (DEXA). However, the risk of osteoporotic fracture is determined collectively by bone mass, architecture and physico-chemistry of the mineral composite building blocks. Thus DEXA scans alone inevitably fail to fully discriminate individuals who will suffer a fragility fracture. This study examines bone at both ultrastructure and microarchitectural levels to provide a detailed material view of bone, and therefore produce a more comprehensive model of osteoporotic fracture risk. Physico-chemical characterisation obtained through X-ray diffraction and infrared analysis indicated significant differences in apatite crystal chemistry and microstructure between fracture and non-fracture groups. Further, this study, through considering the potential correlations between the chemical biomarkers and microarchitectural properties of the bone, has investigated the premise that bone mechanical properties (e.g. fragility) are affected by physicochemical material features.

Keywords: aging, bone quality, hydroxyapatite, osteoporosis, trabecular bone, X-ray diffraction

Introduction

Osteoporosis affects approximately 200 million women around the world. In the UK alone 50% of women will suffer a fracture after the age of 50 [1], a rate which is annually increasing due to the aging population. Osteoporotic fractures often occur in the hip, wrist and vertebrae; although studies have shown hip fractures have the greatest detrimental effect on an individual [2]. Hip fractures result in a significant loss of independence, and sufferers are unable to live without support as they cannot walk unaided or perform many of their daily activities. Worryingly, hip fractures are often associated with increased mortality [3,4], a statistic which is confounded by the asymptomatic nature of osteoporosis. Osteoporosis is often assessed according to an individual's bone mineral density (BMD) [5]. With a decrease in BMD, the risk of fracture is significantly increased [6]. Currently the gold standard for measuring BMD is through the use of dual energy X-ray absorption (DEXA). Unfortunately this method is a poor predictor of fracture, with a study carried out by Wainwright *et al.* showing that 54% of new hip fractures occurred in women who did not have osteoporosis as determined by their BMD [7] and data from the National Osteoporosis Risk Assessment, showed that 82% of post-menopausal women with fractures had bone of 'normal' BMD [8].

The limitations associated with BMD to predict an individual patient's fracture risk is arguably because it does not measure the multiple material factors that contribute to bone strength [9]. Bone strength is a combination of bone density as well as 'bone quality', whereby bone quality refers to bone architecture (i.e. macro and micro) and bone chemistry [9]. A small number of studies (possibly due to the difficulty of obtaining human bone, especially osteoporotic specimens) have shown microarchitectural properties of bone potentially offer a superior way to differentiate between diseased bone (fractured due to osteoporosis or osteoarthritis) when compared to healthy controls (non – fractured tissue) [10 - 12]. Bone chemistry is more complex, with studies often providing contradicting results and conclusions [13 – 18]. Unfortunately, many of the studies which investigate the chemistry of osteoporotic bone are limited by relatively low sample numbers ($n < 6$ for both osteoporotic and 'normal' specimens) [16, 19, 20] and/ or utilise ovariectomised animal models [21, 22]. A more recent study by Boskey [15], investigated the material properties of a large number of cortical and trabecular specimens ($n = 120$) using Fourier transform infrared spectroscopy (FTIR). However, the bone specimens were collected from the iliac crest (as a proxy for fractures at other sites) between 6 months and 5 years after a fracture and such a delay may

1
2 be confounding due to the complexities of remodelling and changes to the bone through
3 aging. Not surprisingly then, the results of many previous studies tend to be conflicting.

4
5 Several previous studies have examined the physicochemical properties of the inorganic bone
6 component (i.e. the hydroxyapatite mineral) characterised by X-ray diffraction (XRD) [13,
7 19, 20] and the organic component (i.e. collagen) as characterised by Raman spectroscopy
8 [23, 24] or Fourier transform infra-red spectroscopy (FTIR) [21, 25, 26]. For example, a
9 recent study of three samples (per group, normal, osteopenic and osteoporotic) by Rollo *et al*
10 suggested a decrease in crystallite size and an increase in lattice microstrain in osteoporotic
11 trabecular bone compared to 'normal' specimens [20]. Satry *et al.* also also reported a
12 decrease in crystallite size in osteoporotic and ovariectomized bone tissue [19]. In contrast,
13 reports such as those of Thompson *et al* [13] and Faibish and Boskey [27] suggested an
14 increase in crystallite size in osteoporotic tissue. These two reports differ however in
15 conclusions regarding the crystal chemistry; Thompson suggesting a decrease in carbonate
16 [13], while Faibish and Boskey [27] argues there is an increase. An increase in both
17 crystallite size and carbonate content was reported by Gadeleta *et al* [14]. Several reports
18 have suggested that there is no significant difference between osteoporotic and normal bone
19 tissue when considering crystallite size [16, 22, 28]. Although a review by Boskey in 2003
20 reported that the general consensus accepts that osteoporotic bone mineral has significantly
21 larger crystallites than the non-osteoporotic counterparts [15], it is evident from the literature
22 this view point is contentious. A more recent study by Boskey *et al.* [18] reported a
23 significant decrease in carbonate to phosphate ratios in that of fractured bone compared to
24 non-fractured cortical bone, suggesting either a decrease in carbonate and/ or an increase in
25 phosphate. No other significant differences were observed for either cortical or trabecular
26 bone. In contrast, McCreadie *et al.* reported an increase in the carbonate to phosphate ratio
27 between specimens collected from women with and without osteoporotic fractures [23].

28
29 Very few studies have examined changes to the hydroxyapatite unit cell parameters (as a
30 proxy for substitutional modifications) of osteoporotic and/or aged bone mineral [28, 29].
31 The major substitution in biological hydroxyapatite is carbonate, which substitutes for the
32 hydroxyl (A – type) and/ or phosphate (B-type) in the crystal lattice or exists on the apatite
33 surface (labile carbonate) [30, 31]. In general, a decrease in 'a' axis and an increase in the 'c'
34 axis lattice parameters has been reported with age [29]. These trends have previously been
35 associated with an increase in B-type carbonate substitution [30]. In contrast other studies
36 were unable to detect differences in the lattice parameters of osteoporotic bone [28]. As a
37
38
39
40
41
42
43
44
45
46
47
48
49
50
51
52
53
54
55
56
57
58
59
60
61
62
63
64
65

1 further bone characteristic measured by FTIR, it has been reported that for osteoporotic
2 tissues the mineral to organic ratio is significantly lower than that of normal bone [14, 25].
3

4 This study reports the physicochemical properties assessed using XRD and FTIR for
5 trabecular bone obtained from the femoral head of individuals who suffered a femoral neck
6 fracture and from a corresponding group where no fracture was reported. Further to this
7 investigation, the data provided an opportunity to explore relationships between the
8 ultrastructure material building blocks and the derived architectural properties. Thus for the
9 first time, the potential effect of the physicochemical properties on the micro architectural
10 properties of bone was investigated. This component of the work only involved the fracture
11 group as relatively large deviations in architecture would be expected in this group.
12
13
14
15
16
17
18
19
20
21

22 **Materials and Methods**

23 *Bone Specimens*

24
25 A sample set of 20 femoral heads were collected from osteoporotic female patients who had
26 suffered trauma fractures at the femoral neck and consequently required hip replacement
27 surgery. Of these 20, the donor's age was available for 16 of the femoral heads. Ethical
28 approval for the collection and use of these specimens was provided by Gloucestershire NHS
29 trust REC. Non-fracture femoral head specimens were collected from 39 female donors
30 within the Melbourne Femur Collection. All donors from this source were coronial cases and
31 had therefore died suddenly and unexpectedly as result of accidents. Ethical approval for the
32 collection and use of these specimens was provided by Melbourne University. Population
33 characteristics for both fracture and non – fracture specimens are provided in Table 1.
34
35
36
37
38
39
40
41
42
43
44
45
46
47
48
49
50
51
52
53
54
55
56
57
58
59
60
61
62
63
64
65

	Fracture	Non-Fracture
Donors	16	39
Age Range (yrs)	59 - 91	20 - 90
Age Mean (yrs)	82.4 ± 6.4	66.1 ± 17.9
Weight Range (kg)	41 - 79	40 - 121
Weight Mean (kg)	61.1 ± 8.9	66.7 ± 19.7
Stature Range (cm)	155 - 173	145 - 169
Stature Mean (cm)	163.9 ± 5.2	159.6 ± 6.7

Table 1: Population characteristics for fracture and non-fracture groups. The standard deviations for all mean values are provided.

Wherein quantitative comparisons are made between groups (fracture and non – fracture), the samples are age matched (70 + years) to avoid any bias arising from differences in age distributions.

Sample Preparation

Sectioning from the femoral head has previously described in detail [32]. Prior to data collections, the specimens were homogenised using a Retsch mixer miller (mm 2000) and a zirconium oxide milling basket and ball. The specimens were cut into smaller sections, to reduce the number of milling cycles and milled for one minute. Between milling, the specimens were allowed to stand for approximately one minute before milling was continued. This limited the potential of the specimen ‘over heating’ during milling, which could potentially cause changes to the mineral microstructure. Once powdered, the specimens were sieved through a stainless steel mesh sieve of 106 µm to ensure a homogenous fine powder sample.

X-ray diffraction (XRD)

The powdered specimens were individually loaded on to low background scattering (off-cut silicon) XRD holders. The bone powder was spiked with a NIST standard silicon powder (REF) to provide an internal standard required for determining accurate lattice parameters.

XRD analysis was carried out using a PANalytical X’Pert PRO Multi-Purpose Diffractometer with Cu K α radiation. A PIXcel strip detector was used to collect data as stepped scans across an angular range of 15 – 80 2 θ (°) (5.90 – 1.20 Å). The count time at each step was equivalent

1 to ~ 1 second. Data was also collected for two further stepped scans under the sample
2 conditions but across an angular range of $23 - 27 2\theta$ ($^{\circ}$) ($3.86 - 3.30 \text{ \AA}$ d-spacing) and $50 -$
3 $55 2\theta$ ($^{\circ}$) ($1.82 - 1.67 \text{ \AA}$ d-spacing), and with a count time at each step equivalent to ~ 3
4 seconds. The two additional stepped scans were collected to provide greater quality data for
5 the 002 and 004 Bragg maxima respectively. This data was used to accurately calculate the
6 full width half maximum (FWHM) of both the 002 and 004 Bragg maxima. The FWHM
7 values were then used to calculate coherence length using the Scherrer equation, as described
8 below. Bruker Topas software (Version 4.1, 2008) was employed to undertake profile fitting
9 of each diffraction profile. This provided quantitative crystallite size and morphology
10 parameters through calculation of the coherence length and structural parameters of the
11 crystal lattice through the lattice parameters.

12
13
14
15
16
17
18
19
20
21 Coherence length was calculated for two orthogonal crystallographic directions, $\langle 00\ell \rangle$ and
22 $\langle 0k0 \rangle$ using the Scherrer equation, which uses the instrument corrected, full width half
23 maximum of the desired peak, as described in [33]. The lattice parameters were calculated
24 from whole pattern fitting refinement of diffraction profiles to obtain the 2θ peak positions.
25 Sample displacement was refined and lattice parameter data corrected accordingly. No unit
26 cell content model was applied and analytical peak shapes were pseudo-Voigt. The data
27 collection, correction and analyses were repeated three times for five randomly selected
28 specimens to assess repeatability.

38 ***Fourier Transform Infrared Spectroscopy (FTIR)***

39
40
41 FTIR analysis was carried out using an attenuated total reflectance – FTIR. ATR-FTIR
42 reduces sample preparation as there is no requirement for preparation of potassium bromide
43 (KBr) pellets and the bone powder can be examined directly. This reduces potential
44 contamination. Approximately 2 mg was used for analysis and three repeats per specimen
45 analysed. FTIR spectra were collected using a Bruker Alpha Platinum ATR and analysis
46 carried out using PerkinElmer Spectrum software. A scan resolution of 4 cm^{-1} and 16 scans
47 was employed for data collection, within a range of $2500 - 400 \text{ cm}^{-1}$.

48
49
50
51
52
53
54
55
56
57
58
59
60
61
62
63
64
65
66
67
68
69
70
71
72
73
74
75
76
77
78
79
80
81
82
83
84
85
86
87
88
89
90
91
92
93
94
95
96
97
98
99
100
101
102
103
104
105
106
107
108
109
110
111
112
113
114
115
116
117
118
119
120
121
122
123
124
125
126
127
128
129
130
131
132
133
134
135
136
137
138
139
140
141
142
143
144
145
146
147
148
149
150
151
152
153
154
155
156
157
158
159
160
161
162
163
164
165
166
167
168
169
170
171
172
173
174
175
176
177
178
179
180
181
182
183
184
185
186
187
188
189
190
191
192
193
194
195
196
197
198
199
200
201
202
203
204
205
206
207
208
209
210
211
212
213
214
215
216
217
218
219
220
221
222
223
224
225
226
227
228
229
230
231
232
233
234
235
236
237
238
239
240
241
242
243
244
245
246
247
248
249
250
251
252
253
254
255
256
257
258
259
260
261
262
263
264
265
266
267
268
269
270
271
272
273
274
275
276
277
278
279
280
281
282
283
284
285
286
287
288
289
290
291
292
293
294
295
296
297
298
299
300
301
302
303
304
305
306
307
308
309
310
311
312
313
314
315
316
317
318
319
320
321
322
323
324
325
326
327
328
329
330
331
332
333
334
335
336
337
338
339
340
341
342
343
344
345
346
347
348
349
350
351
352
353
354
355
356
357
358
359
360
361
362
363
364
365
366
367
368
369
370
371
372
373
374
375
376
377
378
379
380
381
382
383
384
385
386
387
388
389
390
391
392
393
394
395
396
397
398
399
400
401
402
403
404
405
406
407
408
409
410
411
412
413
414
415
416
417
418
419
420
421
422
423
424
425
426
427
428
429
430
431
432
433
434
435
436
437
438
439
440
441
442
443
444
445
446
447
448
449
450
451
452
453
454
455
456
457
458
459
460
461
462
463
464
465
466
467
468
469
470
471
472
473
474
475
476
477
478
479
480
481
482
483
484
485
486
487
488
489
490
491
492
493
494
495
496
497
498
499
500
501
502
503
504
505
506
507
508
509
510
511
512
513
514
515
516
517
518
519
520
521
522
523
524
525
526
527
528
529
530
531
532
533
534
535
536
537
538
539
540
541
542
543
544
545
546
547
548
549
550
551
552
553
554
555
556
557
558
559
560
561
562
563
564
565
566
567
568
569
570
571
572
573
574
575
576
577
578
579
580
581
582
583
584
585
586
587
588
589
590
591
592
593
594
595
596
597
598
599
600
601
602
603
604
605
606
607
608
609
610
611
612
613
614
615
616
617
618
619
620
621
622
623
624
625
626
627
628
629
630
631
632
633
634
635
636
637
638
639
640
641
642
643
644
645
646
647
648
649
650
651
652
653
654
655
656
657
658
659
660
661
662
663
664
665
666
667
668
669
670
671
672
673
674
675
676
677
678
679
680
681
682
683
684
685
686
687
688
689
690
691
692
693
694
695
696
697
698
699
700
701
702
703
704
705
706
707
708
709
710
711
712
713
714
715
716
717
718
719
720
721
722
723
724
725
726
727
728
729
730
731
732
733
734
735
736
737
738
739
740
741
742
743
744
745
746
747
748
749
750
751
752
753
754
755
756
757
758
759
760
761
762
763
764
765
766
767
768
769
770
771
772
773
774
775
776
777
778
779
780
781
782
783
784
785
786
787
788
789
790
791
792
793
794
795
796
797
798
799
800
801
802
803
804
805
806
807
808
809
810
811
812
813
814
815
816
817
818
819
820
821
822
823
824
825
826
827
828
829
830
831
832
833
834
835
836
837
838
839
840
841
842
843
844
845
846
847
848
849
850
851
852
853
854
855
856
857
858
859
860
861
862
863
864
865
866
867
868
869
870
871
872
873
874
875
876
877
878
879
880
881
882
883
884
885
886
887
888
889
890
891
892
893
894
895
896
897
898
899
900
901
902
903
904
905
906
907
908
909
910
911
912
913
914
915
916
917
918
919
920
921
922
923
924
925
926
927
928
929
930
931
932
933
934
935
936
937
938
939
940
941
942
943
944
945
946
947
948
949
950
951
952
953
954
955
956
957
958
959
960
961
962
963
964
965
966
967
968
969
970
971
972
973
974
975
976
977
978
979
980
981
982
983
984
985
986
987
988
989
990
991
992
993
994
995
996
997
998
999
1000

1
2 of the ν_2 carbonate ($890 - 850 \text{ cm}^{-1}$) and ν_3 phosphate bands. Three repeats per specimen
3 were taken to assess repeatability.
4
5
6

7 **Micro Computed Tomography (μ - CT)**

8
9

10 It is hypothesised that correlations between the physicochemical and architectural properties
11 would be more evident than in the non-fracture bone. The architectural properties were
12 obtained from μ - CT, details of which can be found elsewhere [32]. Parameters such as
13 trabecular number (TbN), structure model index (SMI), trabecular thickness (TbTh), bone
14 volume to total volume (BV/ TV) and tissue mineral density (TMD) were previously
15 reported.
16
17
18
19
20
21
22
23

24 **Statistical Analysis**

25

26 Linear regression analysis was carried out to statistically assess correlations between various
27 material characteristics parameters and age for the non-fracture group. A general linear model
28 ANOVA analysis was also undertaken to determine significant differences between the
29 parameters measured for age matched fracture and non-fracture groups. $p < 0.05$ was
30 considered statistically significant for both the linear regression and ANOVA analysis.
31
32
33
34
35
36
37
38

39 **Results**

40

41 This study reports the material quality of trabecular bone from human fracture ($n=16$) and
42 non – fracture specimens ($n = 39$), with the parameters analysed correlated to age. Further,
43 the material quality parameters associated with the fracture specimens have been correlated to
44 the microarchitecture properties (previously reported in [32]). This provides a more
45 comprehensive understanding of how a change in the material chemistry can be associated
46 with and perhaps influence parameters such as trabecular number (TbN), tissue mineral
47 density (TMD), structure model index (SMI) and bone volume to total volume (BV/TV). The
48 average values and associated errors of the material properties derived from both XRD and
49 FTIR analysis are presented in table 2.
50
51
52
53
54
55
56
57
58
59
60
61
62
63
64
65

	All Specimens		Age Matched (70+ yrs)	
	Fracture	Non – Fracture	Fracture	Non – Fracture
N	16	39	15	22
CL 00ℓ (nm)	27.5 \pm 0.6	28.9 \pm 0.3	27.5 \pm 0.6	28.9 \pm 0.4
CL hk0 (nm)	8.24 \pm 0.10	8.21 \pm 0.08	8.23 \pm 0.11	8.30 \pm 0.10
LP ‘a’ axis (Å)	9.402 \pm 0.001	9.406 \pm 0.001	9.402 \pm 0.001	9.406 \pm 0.001
LP ‘c’ axis (Å)	6.896 \pm 0.0006	6.895 \pm 0.002	6.896 \pm 0.0006	6.894 \pm 0.002
Phosphate: Amide	7.10 \pm 0.08	7.06 \pm 0.08	7.05 \pm 0.06	7.19 \pm 0.09
Carbonate: Phosphate	0.020 \pm 0.0004	0.018 \pm 0.0002	0.020 \pm 0.0004	0.018 \pm 0.0003

Table 2: Average values (in bold) and the associated errors (SEM) for the material parameters obtained from XRD and FTIR analysis, for fracture and non-fracture groups.

X-ray Diffraction (XRD)

Coherence length, which provides a quantitative estimate of crystallite size and strain combined (i.e. the total lattice disorder), did not change significantly with age for the non – fracture group in the $\langle 00\ell \rangle$ crystallographic direction, but was found to increase significantly ($p = 0.016$) with age when the $\langle 0k0 \rangle$ direction was considered (Figure 1A). The coherence length values for the fracture group were significantly lower ($p = 0.036$) when age matched to the non – fracture group specimens in the $\langle 00\ell \rangle$ direction (see Table 3). With increasing age, the lattice parameters associated with the ‘a’ axis and ‘c’ axis remain, within experimental errors, constant for the non – fracture group, ranging from approximately 9.40 – 9.41 Å for the ‘a’ axis (Figure 1B) and 6.85 – 6.90 Å for the ‘c’ axis. The ‘a’ axis lattice parameter values for the fracture group are significantly less ($p = 0.001$) than those of the non – fracture group (see Table 3). No significant difference in the ‘c’ axis lattice parameters were observed between the two groups. Note that for characteristics of the non-fracture group that showed no significant age dependence, similar levels of significance were observed when all specimens were included within the ANOVA analyses.

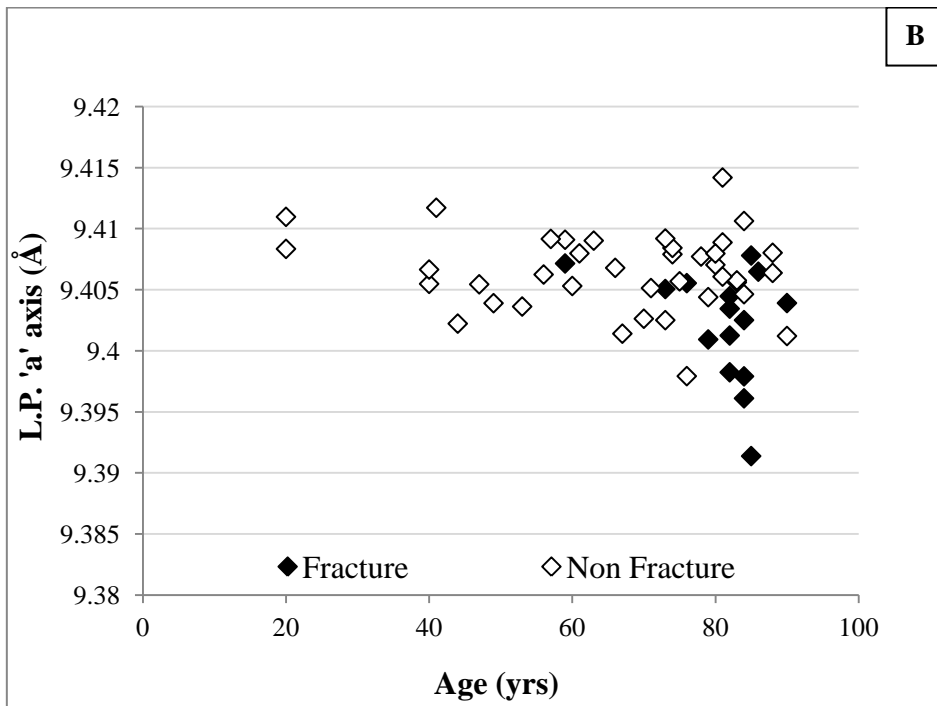
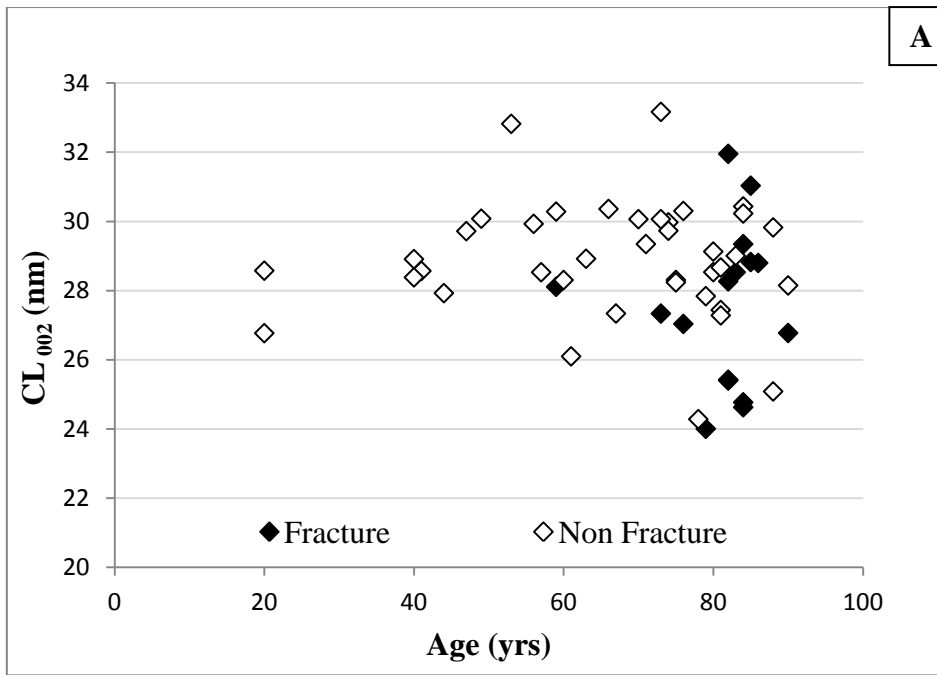


Figure 1: Relationship between X-ray diffraction parameters and age (A: coherence length (CL) values along the 00 l direction vs age, B: 'a' axis lattice parameters vs age), for fracture and non-fracture specimens. Errors have been excluded from the graphs for clarity.

	Linear Regression Analysis			ANOVA	
	Non - Fracture Correlations with Age			Non - Fracture vs Fracture (Age Matched)	
	p - value	R ²	Δ (per 5 yrs)	p - value	Mean Difference (Non Fracture – Fracture)
CL ₀₀₁ (nm)	0.928	0.00	-	0.036	1.4 ± 0.7
CL _{hk0} (nm)	0.016	0.15	0.05 ± 0.02	0.676	-
LP 'a' axis (Å)	0.390	0.02	-	0.001	0.004 ± 0.001
LP 'c' axis (Å)	0.207	0.04	-	0.696	-

Table 3: *Left:* p – values and R² calculated from linear regression statistical analysis when comparing the various XRD material characteristic parameters and age for the non-fracture group. For the parameters where a significant trend was observed, the rate of change (Δ) per 5 years is also reported. *Right:* 3: p – values for age matched ANOVA analysis of fracture (n = 15) and non-fracture groups (n= 22), for each XRD material characteristic parameter. The mean difference between the non-fracture and fracture groups is also reported, for those parameters found to be significantly different (p > 0.05).

Fourier Transform Infrared Spectroscopy (FTIR)

The carbonate to phosphate ratio was found to be significantly greater (p = 0.013) for the fracture group in comparison to the non-fracture group, when age matched. No age related trends were observed for the non – fracture group (Figure 2A). The phosphate to amide ratio values, which indicate an increase in collagen and/ or a reduction in phosphate, are presented in figure 2B for both fracture and non – fracture groups. The variability in the phosphate to amide ratio for the non – fracture group is evident. When age matched, the phosphate: amide values are not significantly different (p = 0.403) for the fracture group in comparison to the non – fracture group. However, with age, an increase in phosphate to amide ratio values was observed (p = 0.023) for the non-fracture group.

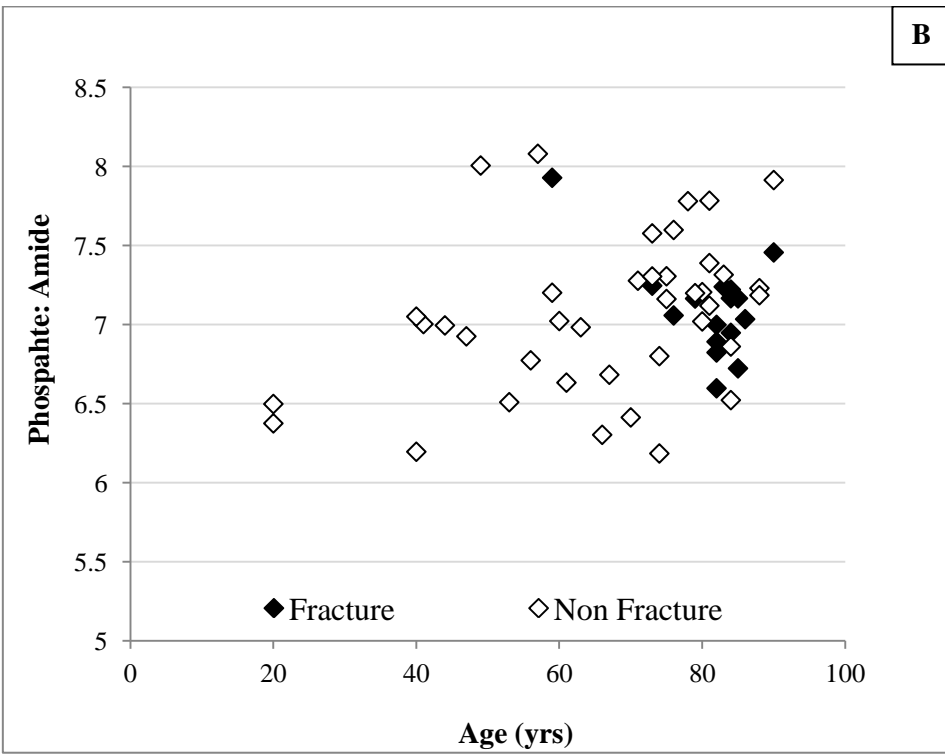
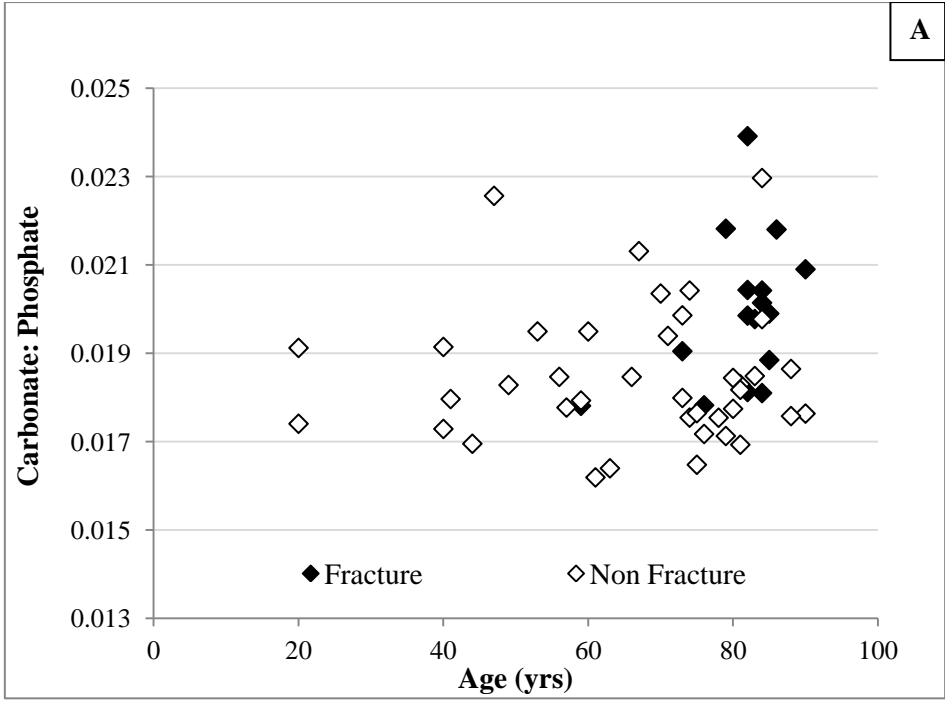


Figure 2: Relationship between FTIR parameters and age (A: carbonate: phosphate values vs age, B: Phosphate: amide values vs age), for fracture and non-fracture specimens. Errors have been excluded from the graphs for clarity.

	Linear Regression Analysis			ANOVA	
	Non - Fracture Correlations with Age			Non - Fracture vs Fracture (Age Matched)	
	p - value	R ²	Δ (per 5 yrs)	p - value	Mean Difference (Non Fracture – Fracture)
Phosphate: Amide	0.023	0.13	0.05 ± 0.02	0.403	-
Carbonate: Phosphate	0.988	0.00	-	0.013	-0.002 ± 0.0005

Table 4: *Left:* p – values and R² calculated from linear regression statistical analysis when comparing the various FTIR material characteristic parameters and age for the non-fracture group. For the parameters where a significant trend was observed, the rate of change (Δ) per 5 years is also reported. *Right:* 3: p – values for age matched ANOVA analysis of fracture (n = 15) and non-fracture groups (n= 22), for each FTIR material characteristic parameter. The mean difference between the non-fracture and fracture groups is also reported, for those parameters found to be significantly different (p > 0.05).

Microarchitecture and Material Characteristics

We have also examined correlations between the material properties and the architectural properties for the fracture group, in order to explore the potential influence bone chemistry may have on the architecture of compromised specimens. There is significant evidence from previous studies that bone mechanical properties (e.g. fragility) are affected by physicochemical material features [14, 38 - 42], although there remains controversy concerning the precise nature and magnitude of such relationships. The composition of apatite is known to markedly affect its crystallite size and shape. For example phosphate substitution by carbonate (bone apatite contains ~5 % wt CO₃²⁻) results in smaller crystallites than the corresponding unsubstituted chemistry [43], as the increase in lattice disorder produces increased solubility of the crystallites [44].

Coherence length

<00ℓ> coherence length values were found to correlate with various microarchitecture parameters previously reported for the fracture group (Figure 3). With increasing coherence

length values, an increase in trabecular thickness (TbTh) ($p = 0.028$, $R^2 = 0.24$, Figure 3A), tissue mineral density (TMD) ($p = 0.006$, $R^2 = 0.35$, Figure 3B) and bone volume to total volume (BV/TV) ($p = 0.036$, $R^2 = 0.22$).

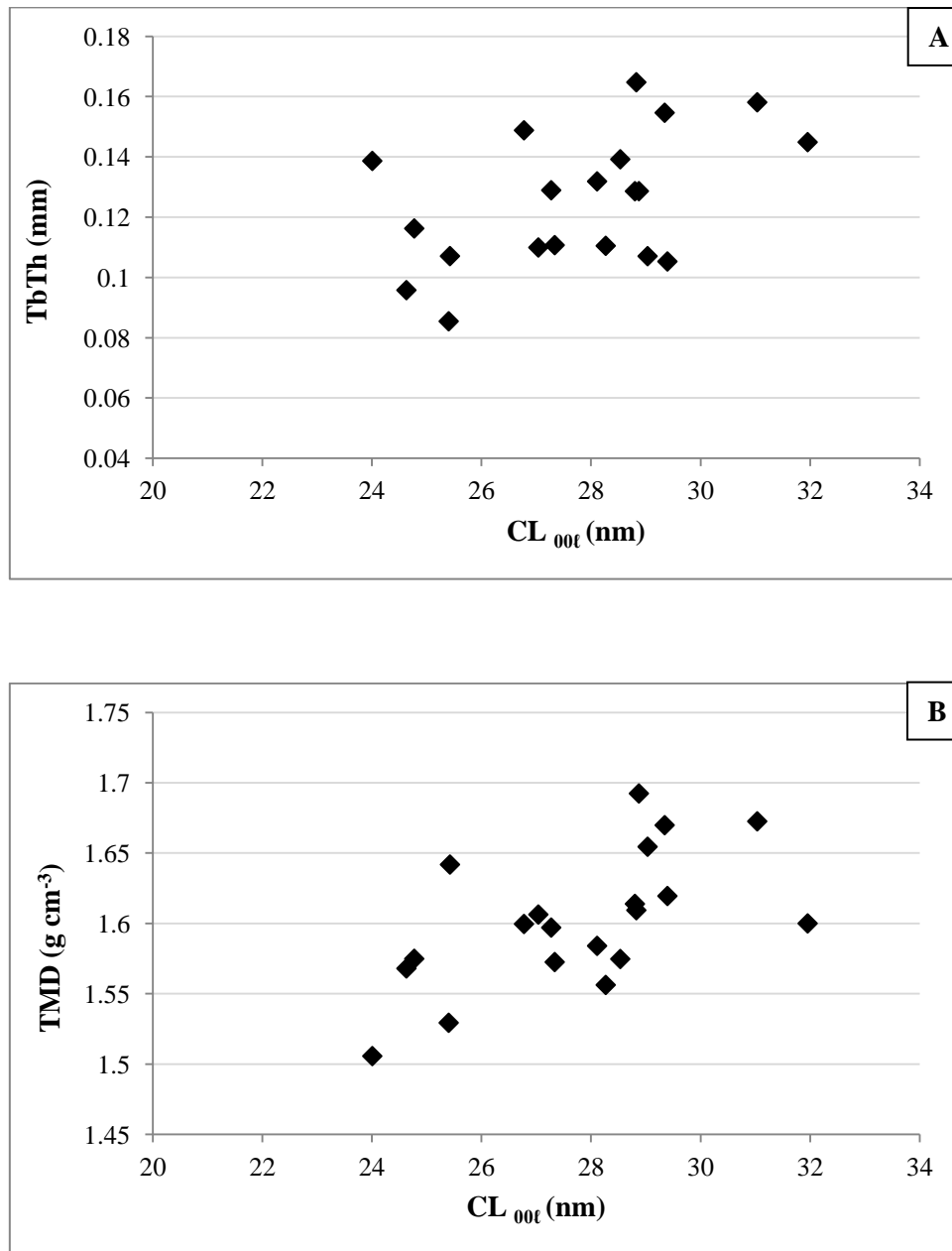


Figure 3: Relationship between microarchitecture properties and coherence length (00l direction), for fracture specimens, A: TbTh vs CL, B: TMD vs CL,. Errors have been excluded from the graphs for clarity.

Discussion

1
2 Although bone performs biologically critical mechanical and homeostatic functions [46] , the
3 relationships between its hierarchical constituents are not well understood. However, in
4 contrast to previous studies where the osteoporotic stage of the bone is unknown (e.g. Ovx)
5 [14, 22, 47], our specimens have fractured and therefore present particularly compromised
6 material. Further the power of some previous studies [16, 19, 20, 28] would be insufficient to
7 demonstrate the significant differences observed within our work. The basis chemical
8 composition (non-stoichiometric hydroxyapatite), crystallises into a variable ultra-structure
9 (nano-crystallites) that together with organic components form the fundamental building
10 blocks of bones microarchitecture. Thus, in order to understand mechanical failures
11 associated with compromised bone tissue such as osteoporotic material, it is crucial to
12 understand the fundamental chemistry of the biological mineral. Current literature focuses on
13 the micro architecture of bone [10 – 12], but few studies have investigated the material
14 crystallographic characteristics of compromised bone mineral [13 – 18]. The potential
15 influence of changes at the nano scale (i.e. in the mineral chemistry) on the micro architecture
16 of human bone has, to the authors' knowledge, not previously been directly considered. X-ray
17 coherent scatter provides information specifically regarding the physicochemical
18 characteristics of bone mineral.
19
20
21
22
23
24
25
26
27
28
29
30
31
32

33
34 Differences in the material properties between osteoporotic and 'normal' material,
35 particularly derived from X-ray diffraction, are not consistent across the literature [13, 19, 20,
36 22, 28, 29]. The absolute values for coherence length from this study are consistent with
37 previously published examinations of human bone [28, 48, 49]. However, the lattice
38 parameters reported herein are significantly less than those reported previously [28, 29]. For
39 this study, an internal reference in the form of silicon was employed to ensure accuracy and
40 our values are consistent with levels of carbonate substitution known to occur in bone [30].
41 Precision was crucial in this study as differences between fracture and non-fracture material
42 were anticipated to be subtle. As previous studies do not use internal references, this could
43 explain the difference in absolute values.
44
45
46
47
48
49
50
51
52

53 We were unable to detect significant changes in $\langle 00l \rangle$ coherence length or lattice parameters
54 with age. A previous study of Handschin and Stern [50] reported an increase in crystal length
55 and perfection up to the age of 25 years old and no significant changes until the age of 50
56 years old, were the average length decreased. The observed changes at 25 years and 50 years
57
58
59
60
61
62
63
64
65

1 old may not have been apparent in the data presented in this study due to study power.
2 Handschin and Stern utilised a significantly greater number of specimens ($n = 117$), across a
3 wider age range (0 – 90 years old). A significant increase in coherence length along the
4 $\langle 0k0 \rangle$ direction, which suggests an increase in crystallite size and perfection, was observed
5 with age in the study reported here.
6
7
8
9

10 When age matched, significant differences between fracture and non-fracture material were
11 demonstrated. The $\langle 00\ell \rangle$ coherence length was found to be significantly lower for the
12 fracture group than the non- fracture group ($p = 0.036$), which is consistent with previous
13 studies [19, 20]. Our study therefore suggests a smaller coherence length corresponds to a
14 material which is more susceptible to fracture, suggesting the mechanical strength would be
15 less than that of non-fractured material. Previous studies have suggested that crystal size is
16 related to mechanical strength [51 - 53], with studies reporting that increased bone mineral
17 crystal size is associated with increased bone fragility [51]. However, after reporting a
18 decrease in crystal thickness with age as crystal length increases, Boskey and Mendelson
19 suggested from their preliminary data that mechanical strength is greater when the average
20 crystallinity is greater [54]. However, Boskey also argued in favour of an optimal situation in
21 which there is a broad distribution of crystal sizes [15] and Fonseca et al. reported that bone
22 strength is favoured by greater mineral crystal size heterogeneity [55]. Further, Chachra et al.
23 [56] reported that a reduction in crystallite size of bone mineral is associated with a decreased
24 load accommodation and increased fracture risk. This is has also been observed in
25 pathologies such as osteoporosis imperfecta [57].
26
27
28
29
30
31
32
33
34
35
36
37
38
39

40 The ‘a’ axis lattice parameter values, which are rarely reported in the literature for bone
41 material, were found to be significantly lower ($p = 0.001$) for the fracture group in
42 comparison to the non-fracture group. In contrast, Mkukuma et al reported no significant
43 difference between osteoporotic material and ‘normal’ tissue when considering lattice
44 parameters [28]. However, the relative low power (low sample numbers) may not have
45 revealed the relatively modest differences ($< 1\%$) between osteoporotic and ‘normal’ tissue.
46 The stoichiometric ‘a’ axis lattice parameter value for hydroxyapatite is reported as 9.42 \AA
47 [29]. The data reported herein suggests non-fracture material is more stoichiometric than the
48 fracture material, and therefore more chemically stable. Changes to lattice parameters values
49 are caused by ionic exchanges and vacancies which induce strain into the lattice. This
50 changes the characteristics of the apatite which are critical to crystallite size and dissolution
51 rate [58]. Greater dissolution rates, for example, will be observed for mineral lattices which
52
53
54
55
56
57
58
59
60
61
62
63
64
65

1
2
3
4
5
6
7
8
9
10
11
12
13
14
15
16
17
18
19
20
21
22
23
24
25
26
27
28
29
30
31
32
33
34
35
36
37
38
39
40
41
42
43
44
45
46
47
48
49
50
51
52
53
54
55
56
57
58
59
60
61
62
63
64
65

are highly strained and therefore less stoichiometric. As osteoporosis is a condition associated with bone loss and perhaps greater turnover, the more soluble lattice structure is probably a more likely state. The reduced lattice parameters calculated for the fracture group is consistent with the carbonate to phosphate ratios calculated with FTIR, as many studies have shown with increasing B –type carbonate, the ‘a’ axis lattice parameter is reduced [30, 59]. No significant difference was observed for the ‘c’ axis lattice parameters between the two groups. Changes to the unit cell through ionic substitutions has previously been shown to have more of an effect on the ‘a’ axis in comparison to the ‘c’ axis [30], which is evident when considering the influence of carbonate substitute on the lattice parameters. LeGeros reported a systematic change in ‘a’ that was 2.5 times that of ‘c’ for an equivalent increase in amount of B-type carbonate substitution [30]. Therefore we propose that the sensitivity of our study is too low to detect corresponding significant changes to the ‘c’ axis.

The material characteristics obtained from FTIR demonstrate an increase in phosphate to amide ratio with increasing age. This may suggest an increase in the amount of phosphate and/or a decrease in collagen (measured through the amide vibrational peak). An increase in mineral content with age has previously been reported [15], as well as an increase in collagen maturity, resulting in a decrease in collagen content [60]. When age matched, the phosphate to amide ratio was not significantly different between the fracture and non-fracture group, although the values for the fracture group were lower. In contrast, previous studies have shown a decrease in the phosphate to amide ratio in both ovariectomised monkeys and osteoporotic human tissue [14, 25, 34, 61], suggesting either a lower mineral content and/ or a greater collagen content. The consensus tends to be that in osteoporotic bone, a decrease in mineral content is observed [14, 15], resulting in a reduction in mechanical strength [55].

Although carbonate incorporation has been reported to increase [50, 62, 63] and decrease [34, 64] with age, no significant correlation with age was observed for the carbonate to phosphate ratio values in this study. This is consistent with [52], who found carbonate incorporation remained constant after 45 years old. When age matched, a significant difference between fracture and non-fracture material was observed for the carbonate to phosphate ratios, with a mean difference of 0.002 ± 0.0004 . The average value for the fracture group was significantly greater in comparison to the non-fracture group. This suggests greater carbonate content in the fracture material in comparison to the non-fracture material and/ or less phosphate. A higher carbonate to phosphate ratio in the fracture material is consistent with previous studies [14, 23, 27], with a study by Boskey suggesting a 8% increase using FTIR [25]. This increase

1
2 is consistent with the data reported here, where a ~ 11% increase in the carbonate to
3 phosphate ratio was observed for the fracture material.

4
5 In general, it is considered that newer bone contains a large quantity of carbonate and is
6 characterised by smaller crystals [31, 65]. In an accelerated turnover system, the consumption
7 rate of the more mature tissue (i.e. that preferentially targeted for remodelling) is enhanced
8 [66]. Crystallite populations then become biased towards reduced average dimensions, larger
9 specific surface areas and greater amounts of carbonate. The data presented here is consistent
10 with this model, as the coherence length values are significantly lower for the fracture
11 material whilst the carbonate to phosphate ratio was significantly greater.
12
13
14
15
16
17

18 This study has also examined relationships between the material characteristics of bone and
19 its corresponding architectural properties, as there is significant evidence from previous
20 studies that bone mechanical properties (e.g. fragility) are affected by physicochemical
21 material features [14, 38 – 42, 51 – 54]. This is the first time these parameters have been
22 compared and the study provides a materials science insight into how bone physicochemistry
23 at the nanoscale potentially influences the architecture at the microscale. The results suggest
24 that material characteristics, in particular the coherence length, potentially have an influence
25 on various micro-architecture properties. Coherence length values are a quantification of
26 crystallite disorder (size and microstrain). An increase in microstrain can indicate ionic
27 substitutions and vacancies. This change can also have an effect on crystallite dimensions and
28 other factors including solubility. Previous studies have shown the solubility of apatite
29 increases as the lattice microstrain is increased [58]. Further, disorder within the apatite
30 lattice, has been proposed as a fundamental contributor to bone mechanical compromise for
31 more than three decades [51] and evidence for this hypothesis continues to be reported [20].
32 In this study, with increasing coherence length values, increases in TbTh, TMD and BV/TV
33 were observed. It is proposed that bone apatite with higher coherence length values represents
34 a more stable, less soluble material and therefore should be associated with increased
35 amounts of bone mineral as reflected by the increase BV/TV, BMD and TbTh.
36
37
38
39
40
41
42
43
44
45
46
47
48
49
50

51 A limited number of fracture and non-fracture material from age matched male donors (7)
52 were also examined. It was found that the phosphate to mineral ratio values were
53 significantly greater for the fracture group, suggesting a reduction in collagen and/ or an
54 increase in phosphate. In contrast, the carbonate to phosphate ratio values between the two
55 groups was not significantly different. The tissue mineral density (TMD), was also
56
57
58
59
60
61
62
63
64
65

1 significantly different between fracture material collected from female and male donors;
2 TMD was greater for the male specimens. This difference may be due to fundamental
3 compositional differences between the female and male fracture material. For example, if the
4 carbonate content is significantly greater in the female fracture group then this would reduce
5 the apatite density (therefore TMD). Stoichiometric hydroxyapatite, $\sim 3.2 \text{ g cm}^{-3}$ [67], has
6 been shown to decrease with the incorporation of increasing amounts of carbonate [68, 69].
7 Reducing the amount of carbonate by $\sim 50\%$ produces an increase in density by $\sim 15\%$.
8 Further, the phosphate to amide ratio was significantly greater for the male fracture material
9 suggesting an increase in phosphate and/ or a decrease in collagen, both of which would
10 modify TMD values. An increase in phosphate would result in a more stoichiometric mineral,
11 resulting in an increase in density, whilst a decrease in collagen, would result in an average
12 increase in TMD. The differences in the fracture group between males and females, as
13 previously hypothesised [70], maybe due to remodelling differences caused by different
14 hormonal changes in men and women.
15
16
17
18
19
20
21
22
23
24
25
26

27 **Conclusion**

28
29 The principal main aim of this study was to investigate bone ‘quality’ in terms of mineral
30 chemistry and organic content of fractured and non-fractured human material. Age related
31 changes for the non-fracture material were also investigated. For the first time, the
32 relationship between the material characteristics and the micro architecture parameters was
33 examined. As shown through statistical analysis, the coherence length ($\langle 00\ell \rangle$), ‘a’ axis
34 lattice parameters and carbonate to phosphate ratio values (when age matched) were
35 significantly different between fracture and non-fracture material from female donors. The
36 study has also shown an increase in crystallite size and perfection ($[0k0]$) as well as an
37 increase in the amount of phosphate and/or a decrease in collagen occurs with age for non-
38 fracture material. It is proposed the data reported here suggests osteoporosis may not simply
39 be an accelerated aging process when considering mineral chemistry and organic content, but
40 there are fundamental chemical differences between fracture and non-fracture material not
41 found with age. It is interesting to speculate that the mineral properties of bone at the
42 ultrastructure level may influence the micro architectural properties of trabecular bone. A
43 preliminary investigation into the material properties of fractured and non-fractured material
44 from male donors, although not presented here, suggested differences in the material quality
45 between fracture males and females. It is proposed these differences translate through to
46
47
48
49
50
51
52
53
54
55
56
57
58
59
60
61
62
63
64
65

1 measured TMD values and potentially highlight differences in bone remodelling between
2 fracture males and females.
3
4
5
6

7 **Acknowledgements**

8
9 This programme of work is funded by an Engineering and Physical Sciences Research
10 Council (grant: EP/K020196/1 Point-of-Care High Accuracy Fracture Risk Prediction). The
11 authors acknowledge the support provided by the UK Department of Transport under the
12 BOSCOS (Bone Scanning for Occupant Safety) project for which the human material was
13 obtained in the Gloucester and Cheltenham NHS Trust hospitals under ethical consent
14 (BOSCOS - Mr. Curwen CI REC ref. 01/179G) and were from individuals who either
15 consented themselves or where their next of kin signed an informed consent. The consents
16 pertained to the use in relation to diagnostic purposes and basic bone research. The authors
17 also recognise support from the Victorian Institute of Forensic Pathology, which later
18 changed its name to the Victorian Institute of Forensic Medicine (VIFM). All donors from
19 this source were coronial cases and had therefore died suddenly and unexpectedly frequently
20 as result of accidents. Permission to remove the tissue for research was obtained from the
21 next of kin in strict accordance with Australian National Health and Medical Research
22 Council guidelines and prevailing local legislation. The approach to the families was made by
23 trained transplant coordinators who also administered a limited questionnaire to investigate
24 the medical history of the deceased where this was known. Ethics approval was sought and
25 obtained for our program of studies into age-related changes to bone both at the VIFM and at
26 the University of Melbourne. Later, when material was no longer being collected at autopsy,
27 responsibility for ethical oversight was transferred exclusively to The University of
28 Melbourne on 28th April 2011 ethics ID 1135392. This is continuing.
29
30
31
32
33
34
35
36
37
38
39
40
41
42
43
44
45
46
47
48
49
50
51
52
53
54
55
56
57
58
59
60
61
62
63
64
65

References

- 1
2 [1] Van Staa TP, Dennison EM, Leufkens HG, Cooper C. Epidemiology of fractures in
3 England and Wales. *Bone*. 2001 Dec 31;29(6):517-22.
4
5
6 [2] Keene GS, Parker MJ, Pryor GA. Mortality and morbidity after hip fractures. *Bmj*. 1993
7 Nov 13;307(6914):1248-50.
8
9
10 [3] Cooper C, Atkinson EJ, Jacobsen SJ, O'Fallon WM, Melton LJ. Population-based study
11 of survival after osteoporotic fractures. *American Journal of Epidemiology*. 1993 May
12 1;137(9):1001-5.
13
14 [4]. Leibson CL, Tosteson AN, Gabriel SE, Ransom JE, Melton LJ. Mortality, disability, and
15 nursing home use for persons with and without hip fracture: a population-based study.
16 *Journal of the American Geriatrics Society*. 2002 Oct 1;50(10):1644-50.
17
18 [5] Kanis JA, Delmas P, Burckhardt P, Cooper C, Torgerson DO. Guidelines for diagnosis
19 and management of osteoporosis. *Osteoporosis International*. 1997 Jul 1;7(4):390-406.
20
21 [6] Marshall D, Johnell O, Wedel H. Meta-analysis of how well measures of bone mineral
22 density predict occurrence of osteoporotic fractures. *Bmj*. 1996 May 18;312(7041):1254-9.
23
24 [7] Wainwright SA, Marshall LM, Ensrud KE, Cauley JA, Black DM, Hillier TA, Hochberg
25 MC, Vogt MT, Orwoll ES. Hip fracture in women without osteoporosis. *The Journal of*
26 *Clinical Endocrinology & Metabolism*. 2005 May 1;90(5):2787-93.
27
28 [8] Siris ES, Chen YT, Abbott TA, Barrett-Connor E, Miller PD, Wehren LE, Berger ML.
29 Bone mineral density thresholds for pharmacological intervention to prevent fractures.
30 *Archives of Internal Medicine*. 2004 May 24;164(10):1108-12.
31
32 [9] .Farlay, D., Boivin, G.: Bone Mineral Quality. InTech Press, 2012. doi:[10.5772/29091](https://doi.org/10.5772/29091)
33
34 [10] Kijowski R, Tuite M, Kruger D, Munoz Del Rio A, Kleerekoper M, Binkley N.
35 Evaluation of trabecular microarchitecture in nonosteoporotic postmenopausal women with
36 and without fracture. *Journal of Bone and Mineral Research*. 2012 Jul 1;27(7):1494-500.
37
38 [11] Milovanovic P, Djonic D, Marshall RP, Hahn M, Nikolic S, Zivkovic V, Amling M,
39 Djuric M. Micro-structural basis for particular vulnerability of the superolateral neck
40 trabecular bone in the postmenopausal women with hip fractures. *Bone*. 2012 Jan
41 31;50(1):63-8.
42
43 [12] Djuric M, Zagorac S, Milovanovic P, Djonic D, Nikolic S, Hahn M, Zivkovic V,
44 Bumbasirevic M, Amling M, Marshall RP. Enhanced trabecular micro-architecture of the
45 femoral neck in hip osteoarthritis vs. healthy controls: a micro-computer tomography study in
46 postmenopausal women. *International Orthopaedics*. 2013 Jan 1;37(1):21-6.
47
48
49
50
51
52
53
54
55
56
57
58
59
60
61
62
63
64
65

- 1
2
3
4
5
6
7
8
9
10
11
12
13
14
15
16
17
18
19
20
21
22
23
24
25
26
27
28
29
30
31
32
33
34
35
36
37
38
39
40
41
42
43
44
45
46
47
48
49
50
51
52
53
54
55
56
57
58
59
60
61
62
63
64
65
- [13] Thompson DD, Posner AS, Laughlin WS, Blumenthal NC. Comparison of bone apatite in osteoporotic and normal Eskimos. *Calcified Tissue International*. 1983 Dec 1;35(1):392-3.
- [14] Gadeleta SJ, Boskey AL, Paschalis E, Carlson C, Menschik F, Baldini T, Peterson M, Rimnac CM. A physical, chemical, and mechanical study of lumbar vertebrae from normal, ovariectomized, and nandrolone decanoate-treated cynomolgus monkeys (*Macaca fascicularis*). *Bone*. 2000 Oct 31;27(4):541-50.
- [15] Boskey A. Bone mineral crystal size. *Osteoporosis International*. 2003 Sep 1;14:S16-21.
- [16] Rubin MA, Jasiuk I, Taylor J, Rubin J, Ganey T, Apkarian RP. TEM analysis of the nanostructure of normal and osteoporotic human trabecular bone. *Bone*. 2003 Sep 30;33(3):270-82.
- [17] Yerramshetty J, Akkus O (2013) Changes in cortical bone mineral and microstructure with aging and osteoporosis. In: Silva MJ (ed) *Skeletal Aging and Osteoporosis. Biomechanics and Mechanobiology*. Springer, Heidelberg, pp 105 – 131
- [18] Boskey AL, Donnelly E, Boskey E, Spevak L, Ma Y, Zhang W, Lappe J, Recker RR. Examining the Relationships Between Bone Tissue Composition, Compositional Heterogeneity, and Fragility Fracture: A Matched Case-Controlled FTIRI Study. *Journal of Bone and Mineral Research*. 2015 Dec 1.
- [19] Sastry TP, Chandrasekaran A, Sundaraseelan J, Ramasastry M, Sreedhar R. Comparative study of some physico-chemical characteristics of osteoporotic and normal human femur heads. *Clinical Biochemistry*. 2007 Aug 31;40(12):907-12.
- [20] Rollo JM, Boffa RS, Cesar R, Schwab DC, Leivas TP. Assessment of Trabecular Bones Microarchitectures and Crystal Structure of Hydroxyapatite in Bone Osteoporosis with Application of the Rietveld Method. *Procedia Engineering*. 2015 Dec 31;110:8-14.
- [21] Huang RY, Miller LM, Carlson CS, Chance MR. In situ chemistry of osteoporosis revealed by synchrotron infrared microspectroscopy. *Bone*. 2003 Oct 31;33(4):514-21.
- [22] Lundon K, Dumitriu M, Grynepas M. The long-term effect of ovariectomy on the quality and quantity of cancellous bone in young macaques. *Bone and mineral*. 1994 Feb 28;24(2):135-49.
- [23] McCreadie BR, Morris MD, Chen TC, Rao DS, Finney WF, Widjaja E, Goldstein SA. Bone tissue compositional differences in women with and without osteoporotic fracture. *Bone*. 2006 Dec 31;39(6):1190-5.

- 1
2
3
4
5
6
7
8
9
10
11
12
13
14
15
16
17
18
19
20
21
22
23
24
25
26
27
28
29
30
31
32
33
34
35
36
37
38
39
40
41
42
43
44
45
46
47
48
49
50
51
52
53
54
55
56
57
58
59
60
61
62
63
64
65
- [24] Paschalis EP, Fratzl P, Gamsjaeger S, Hassler N, Brozek W, Eriksen EF, Rauch F, Glorieux FH, Shane E, Dempster D, Cohen A. Aging Versus Postmenopausal Osteoporosis: Bone Composition and Maturation Kinetics at Actively-Forming Trabecular Surfaces of Female Subjects Aged 1 to 84 Years. *Journal of Bone and Mineral Research*. 2015 Sep 1.
- [25] Boskey AL, DiCarlo E, Paschalis E, West P, Mendelsohn R. Comparison of mineral quality and quantity in iliac crest biopsies from high-and low-turnover osteoporosis: an FT-IR microspectroscopic investigation. *Osteoporosis International*. 2005 Dec 1;16(12):2031-8.
- [26] Ruppel ME, Burr DB, Miller LM. Chemical makeup of microdamaged bone differs from undamaged bone. *Bone*. 2006 Aug 31;39(2):318-24.
- [27] Faibish D, Ott SM, Boskey AL. Mineral changes in osteoporosis a review. *Clinical Orthopaedics and Related Research*. 2006 Feb;443:28.
- [28] Mkukuma LD, Imrie CT, Skakle JM, Hukins DW, Aspden RM. Thermal stability and structure of cancellous bone mineral from the femoral head of patients with osteoarthritis or osteoporosis. *Annals of the Rheumatic Diseases*. 2005 Feb 1;64(2):222-5.
- [29] Handschin RG, Stern WB. Crystallographic lattice refinement of human bone. *Calcified Tissue International*. 1992 Aug 1;51(2):111-20.
- [30] Zapanta-LeGeros R. Effect of carbonate on the lattice parameters of apatite. *Nature*, 1965 April, 206, 403 – 404, doi:10.1038/206403a0
- [31] Rey C, Collins B, Goehl T, Dickson IR, Glimcher MJ. The carbonate environment in bone mineral: a resolution-enhanced Fourier transform infrared spectroscopy study. *Calcified Tissue International*. 1989 May 1;45(3):157-64.
- [32] Greenwood C, Clement JG, Dicken AJ, Evans JP, Lyburn ID, Martin RM, Rogers KD, Stone N, Adams G, Zioupos P. The micro-architecture of human cancellous bone from fracture neck of femur patients in relation to the structural integrity and fracture toughness of the tissue. *Bone Reports*. 2015 Dec 31;3:67-75.
- [33] E.F. Kaelble (Ed.), *Handbook of X-rays for Diffraction, Emission, Absorption, and Microscopy*, McGraw-Hill, New York, 1967, pp. 17–25.
- [34] Paschalis EP, Betts F, DiCarlo E, Mendelsohn R, Boskey AL. FTIR microspectroscopic analysis of normal human cortical and trabecular bone. *Calcified Tissue International*. 1997 Dec 1;61(6):480-6.
- [35] Paschalis EP, Mendelsohn R, Boskey AL. Infrared assessment of bone quality: a review. *Clinical Orthopaedics and Related Research*. 2011 Aug 1;469(8):2170-8.
- [36] Pienkowski D, Doers TM, Monier-Faugere MC, Geng Z, Camacho NP, Boskey AL, Malluche HH. Calcitonin alters bone quality in beagle dogs. *Journal of Bone and Mineral Research*. 1997 Nov 1;12(11):1936-43.

- 1
2
3 [37] Bohic S, Heymann D, Pouëzat JA, Gauthier O, Daculsi G. Transmission FT-IR
4
5
6 [38] Turan B, Bayari S, Balcik C, Severcan F, Akkas N. A biomechanical and spectroscopic
7
8
9 study of bone from rats with selenium deficiency and toxicity. *Biometals*. 2000 Jun
10
11 [39] Kohles SS, Martinez DA. Elastic and physicochemical relationships within cortical
12
13
14 [40] Freeman JJ, Wopenka B, Silva MJ, Pasteris JD. Raman spectroscopic detection of
15
16
17 changes in bioapatite in mouse femora as a function of age and in vitro fluoride treatment.
18
19 [41] Camacho NP, Hou L, Toledano TR, Ilg WA, Brayton CF, Raggio CL, Root L, Boskey
20
21
22 AL. The material basis for reduced mechanical properties in oim mice bones. *Journal of Bone
23
24 and Mineral Research*. 1999 Feb 1;14(2):264-72.
25
26 [42] Landete-Castillejos T, Currey JD, Estevez JA, Gaspar-López E, Garcia A, Gallego L.
27
28 Influence of physiological effort of growth and chemical composition on antler bone
29
30
31 mechanical properties. *Bone*. 2007 Nov 30;41(5):794-803.
32
33 [43] Yao F, LeGeros RZ. Carbonate and fluoride incorporation in synthetic apatites:
34
35
36 Comparative effect on physico-chemical properties and in vitro bioactivity in fetal bovine
37
38
39 serum. *Materials Science and Engineering: C*. 2010 Apr 6;30(3):423-30.
40
41
42 [44] Tang R, Henneman ZJ, Nancollas GH. Constant composition kinetics study of
43
44
45 carbonated apatite dissolution. *Journal of Crystal Growth*. 2003 Mar 31;249(3):614-24.
46
47 [45] Baig AA, Fox JL, Young RA, Wang Z, Hsu J, Higuchi WI, Chhetry A, Zhuang H,
48
49
50
51 Otsuka M. Relationships among carbonated apatite solubility, crystallite size, and microstrain
52
53
54 parameters. *Calcified Tissue International*. 1999 May 1;64(5):437-49.
55
56 [46] Florencio-Silva R, Sasso GR, Sasso-Cerri E, Simões MJ, Cerri PS. Biology of bone
57
58
59 tissue: structure, function, and factors that influence bone cells. *BioMed Research
60
61
62 International*. 2015 Jan 1;2015.
63
64 [47] Orkoula MG, Vardaki MZ, Kontoyannis CG. Study of bone matrix changes induced by
65
osteoporosis in rat tibia using raman spectroscopy. *Vibrational Spectroscopy*. 2012 Nov
30;63:404-8.
- [48] Holden JL, Clement JG, Phakey PP. Age and temperature related changes to the
ultrastructure and composition of human bone mineral. *Journal of Bone and Mineral
Research*. 1995 Sep 1;10(9):1400-9.

1 [49] Beckett S, Rogers KD, Clement JG. Inter-Species Variation in Bone Mineral Behavior
2 upon Heating. *Journal of Forensic Sciences*. 2011 May 1;56(3):571-9.

3
4 [50] Handschin RG, Stern WB. X-ray diffraction studies on the lattice perfection of human
5 bone apatite (Crista iliaca). *Bone*. 1995 Apr 30;16(4):S355-63.

6
7
8
9 [51] Chatterji S, Wall JC, Jeffery JW. Age-related changes in the orientation and particle size
10 of the mineral phase in human femoral cortical bone. *Calcified Tissue International*. 1981
11 Dec 1;33(1):567-74.

12
13
14
15 [52] Akkus O, Adar F, Schaffler MB. Age-related changes in physicochemical properties of
16 mineral crystals are related to impaired mechanical function of cortical bone. *Bone*. 2004 Mar
17 31;34(3):443-53.

18
19
20 [53] Turner CH, Garetto LP, Dunipace AJ, Zhang W, Wilson ME, Gryn timer MD, Chachra D,
21 McClintock R, Peacock M, Stookey GK. Fluoride treatment increased serum IGF-1, bone
22 turnover, and bone mass, but not bone strength, in rabbits. *Calcified Tissue International*.
23 1997 Jul 1;61(1):77-83.

24
25
26
27 [54] Boskey A, Mendelsohn R. Infrared analysis of bone in health and disease. *Journal of*
28 *Biomedical Optics*. 2005 May 1;10(3):031102-9.

29
30 [55] Fonseca H, Moreira-Gonçalves D, Coriolano HJ, Duarte JA. Bone quality: The
31 determinants of bone strength and fragility. *Sports Medicine*. 2014 Jan 1;44(1):37-53.

32
33
34 [56] Chachra D, Turner CH, Dunipace AJ, Gryn timer MD. The effect of fluoride treatment on
35 bone mineral in rabbits. *Calcified Tissue International*. 1999 Apr 1;64(4):345-51.

36
37
38 [57] Vetter U, Eanes ED, Kopp JB, Termine JD, Robey PG. Changes in apatite crystal size
39 in bones of patients with osteogenesis imperfecta. *Calcified Tissue International*. 1991 Jul
40 1;49(4):248-50.

41
42
43 [58] Wopenka B, Pasteris JD. A mineralogical perspective on the apatite in bone. *Materials*
44 *Science and Engineering: C*. 2005 Apr 28;25(2):131-43.

45
46
47 [59] Nelson DG, Featherstone JD. Preparation, analysis, and characterization of carbonated
48 apatites. *Calcified Tissue International*. 1981 Dec;34:S69-81.

49
50 [60] Bailey AJ, Sims TJ, Ebbesen EN, Mansell JP, Thomsen JS, Mosekilde L. Age-related
51 changes in the biochemical properties of human cancellous bone collagen: relationship to
52 bone strength. *Calcified tissue international*. 1999 Sep 1;65(3):203-10.

53
54
55 [61] Burket JC, Brooks DJ, MacLeay JM, Baker SP, Boskey AL, van der Meulen MC.
56 Variations in nanomechanical properties and tissue composition within trabeculae from an
57 ovine model of osteoporosis and treatment. *Bone*. 2013 Jan 31;52(1):326-36.

58
59
60
61
62
63
64
65

1 [62] Legros R, Balmain N, Bonel G. Age-related changes in mineral of rat and bovine
2 cortical bone. *Calcified Tissue International*. 1987 Sep 1;41(3):137-44.

3 [63] Rey C, Renugopalakrishnan V, Collins B, Glimcher MJ. Fourier transform infrared
4 spectroscopic study of the carbonate ions in bone mineral during aging. *Calcified Tissue*
5 *International*. 1991 Jul 1;49(4):251-8.

6 [64] Ouyang H, Sherman PJ, Paschalis EP, Boskey AL, Mendelsohn R. Fourier transform
7 infrared microscopic imaging: effects of estrogen and estrogen deficiency on fracture healing
8 in rat femurs. *Applied Spectroscopy*. 2004 Jan 1;58(1):1-9.

9 [65] Miller LM, Vairavamurthy V, Chance MR, Mendelsohn R, Paschalis EP, Betts F,
10 Boskey AL. In situ analysis of mineral content and crystallinity in bone using infrared micro-
11 spectroscopy of the ν_4 PO₄³⁻ vibration. *Biochimica et Biophysica Acta (BBA)-General*
12 *Subjects*. 2001 Jul 2;1527(1):11-9.

13 [66] Clarke B. Normal bone anatomy and physiology. *Clinical Journal of the American*
14 *Society of Nephrology*. 2008 Nov 1;3(Supplement 3):S131-9.

15 [67] Posner AS, Perloff A, Diorio AF. Refinement of the hydroxyapatite structure. *Acta*
16 *Crystallographica*. 1958 Apr 10;11(4):308-9.

17 [68] El Feki H, Savariault JM, Salah AB, Jemal M. Sodium and carbonate distribution in
18 substituted calcium hydroxyapatite. *Solid State Sciences*. 2000 Sep 1;2(5):577-86.

19 [69] Wilson RM, Elliott JC, Dowker SE, Smith RI. Rietveld structure refinement of
20 precipitated carbonate apatite using neutron diffraction data. *Biomaterials*. 2004 May
21 31;25(11):2205-13.

22 [70] Seeman E. Pathogenesis of bone fragility in women and men. *The Lancet*. 2002 May
23 25;359(9320):1841-50.

24
25
26
27
28
29
30
31
32
33
34
35
36
37
38
39
40
41
42
43
44
45
46
47
48
49
50
51
52
53
54
55
56
57
58
59
60
61
62
63
64
65